


Isotopic and hydrogeochemical characterization of high-altitude karst aquifers in complex geological settings. The Ordesa and Monte Perdido National Park (Northern Spain) case study

 J. Lambán^a

javier.lamban@igme.es

J. Jódar^b

jorge.jodar@upc.edu

E. Custodio^b

emilio.custodio@upc.edu

A. Soler^c

albertsoler@ub.edu

G. Sapriza^d

g.sapriza@usask.ca

R. Soto^a

r.soto@igme.es

^aGeological Survey of Spain (IGME), [Spain](#)

^bDepartment of Geotechnical Engineering and Geosciences, Technical University of Catalonia (UPC), Barcelona, Spain

^cGrup de Mineralogia Aplicada i Medi Ambient, Departament Cristal·lografia Mineralogia i Dipòsits Minerals, Facultat de Geologia, Universitat de Barcelona (UB), [Spain](#)

^dGlobal Institute for Water Security, National Hydrology Research Centre, Canada

Editor: D. Barcelo

Abstract

The Ordesa and Monte Perdido National Park, located in the Southern Pyrenees, constitutes the highest karst system in Western Europe. No previous studies regarding its geochemical and isotopic groundwater characterization are available in this area. This work presents the results of field and sampling campaigns carried out between July 2007 and September 2013. The groundwater presents high calcium bicarbonate contents due to the occurrence of upper Cretaceous and lower Paleocene–Eocene carbonate materials in the studied area. Other relevant processes include dissolution of anhydrite and/or gypsum and incongruent dissolution of Mg-limestone and dolomite. The water stable isotopes ($\delta^{18}\text{O}$, $\delta^2\text{H}$) show that the oceanic fronts from the Atlantic Ocean are responsible for the high levels of precipitation. In autumn, winter, and spring, a deuterium excess is found in the recharge water, which could be related to local atmospheric transport of low-altitude snow sublimation vapour and its later condensation on the snow surface at higher altitude, where recharge is mostly produced. The recharge zones are mainly between 2500 m and 3200 m a.s.l. The tritium content of the water suggests short groundwater transit times. The isotopic composition of dissolved sulphate points to the existence of regional fluxes mixed with local discharge in some of the springs. This work highlights the major role played by the altitude difference between the recharge and discharge zones in controlling the chemistry and the vertical variability of the isotopic composition in high-altitude karst aquifers.

Keywords: Environmental isotopes; Snow sublimation; Deuterium excess; Karst hydrology; Alpine hydrology; Parque Nacional Ordesa y Monte Perdido

1 Introduction

The Ordesa and Monte Perdido National Park (PNOMP), located in the Southern Pyrenees, is the highest calcareous massif in Western Europe. Its landscape derives mainly from glacial and karst processes. Its altitude (3355 m a.s.l. at its highest point) and large altitudinal differences between the recharge and discharge points (e.g., 689 m in the Fuen dero Baño spring) allow the PNOMP to be used as a natural laboratory to analyse the hydrogeology of high-altitude karsts and how the isotopic and hydrogeochemical features of groundwater vary with altitude.

Karst aquifers present characteristics that make them very different from other aquifers, such as high heterogeneity generated by the endokarstic network, high velocities of water flow and short residence times (e.g., Kiraly, 1997; Motyka, 1998). When karst aquifers are located in high-altitude mountain zones, their hydrogeologic behaviour is also influenced by other variables that include large thermal vertical gradients, extremely short response times to precipitation events and snow melt dynamics that control aquifer recharge during the winter and spring seasons (Gremaud et al, 2009; Gremaud and Goldscheider, 2010). In these cases, environmental isotopes represent a powerful tool to characterize their hydrogeology (Collins and Gordon, 1981). Thus, recharge zones can be defined by using $\delta^{18}\text{O}$ and $\delta^2\text{H}$ contents (Araguás-Araguás et al., 2000; Gonfiantini et al., 2001). Tritium (^3H) can be used either to separate base flow from snow melt runoff or to estimate groundwater transit times (Boronina et al., 2005; Gustafson, 2007). The analysis of $\delta^{34}\text{S}_{\text{SO}_4}$ and $\delta^{18}\text{O}_{\text{SO}_4}$ in spring waters can provide information on the origin of the solutes and on the water rock interaction processes (Schaefer and Uzdowski, 1992; González-Fernández et al., 2009).

Despite the importance of high-altitude karst aquifers as recharge areas for water resources (e.g., the Alps, the Pyrenees, and the Carpathians), the hydrogeological characterization of these complex systems has not been extensively studied. Here, the first hydrogeological characterization of the PNOMP is presented. The objectives are twofold: to analyse the groundwater geochemistry and isotopic content ($\delta^{18}\text{O}$ and $\delta^2\text{H}$, $\delta^{34}\text{S}_{\text{SO}_4}$, $\delta^{18}\text{O}_{\text{SO}_4}$ and ^3H) and to determine the role played by the high altitude and low temperature conditions in the hydrogeological behaviour of karst systems.

2 The study area

The PNOMP is located in the central sector of the Southern Pyrenees, one of the highest and largest mountain chains of the Iberian Peninsula (Fig. 1). The PNOMP has several peaks over 3000 m a.s.l., with the Monte Perdido (3355 m a.s.l.) its highest point. Its lowest point, at 689 m a.s.l., is located in the Fuen dero Baño spring (site 22; Fig. 1). The PNOMP shows an alpine mountain landscape resulting mainly from a heterogeneous, karstified landscape with numerous karren fields, caves, sinkholes and fissures and from glacial processes as shown by the long and deep, U-shaped, glacial valleys of Ordesa, Añisclo, Escuaín and Pineta (Fig. 1).

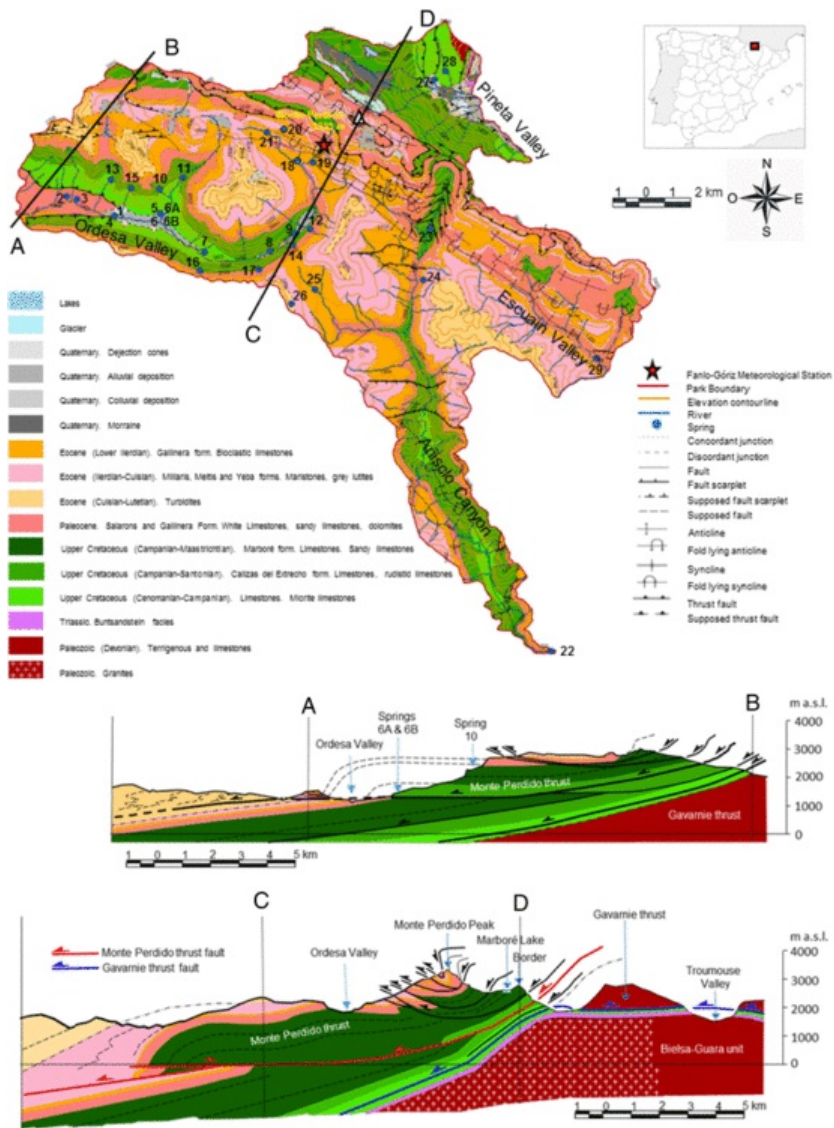


Fig. 1 Location, geological map of the Ordesa and Monte Perdido National Park and geological cross sections A–B and C–D (modified from Seguret, 1972 and IGME-OAPN, 2013). Blue points correspond to the sampled springs. The numbers correspond to those in Table 1. [\[For interpretation of the references to colour in this figure legend, the reader is referred to the web version of this article.\]](#)

The Pyrenean range is a roughly E–W-trending Alpine belt resulting from the collision between the Iberian and European plates (e.g., Muñoz, 1992). It is approximately 1000 km long and 175 to 250 km wide. The rocks outcropping along the belt can be grouped into two categories: the pre-Hercynian basement (with Precambrian to middle-upper Carboniferous rocks) and the post-Hercynian cover (from Stephanian up to Tertiary rocks). The pre-Hercynian rocks in the Pyrenees have been affected by two major orogenic events: the Hercynian (late Carboniferous, pre-Stephanian) and the Alpine (Eocene–Oligocene) orogenies. The Hercynian tectonics are characterized by a regional foliation related to WNW–ESE-trending folds, N–S- to NE–SW-trending shear zones, and several E–W thrust sheets (Carreras and Santanach, 1983). This structural framework was later inherited when the modern Pyrenees were formed during the Alpine orogeny (Parish, 1984; Muñoz et al., 1986). From Late Cretaceous to Miocene times, an asymmetric, doubly vergent orogenic wedge developed, characterized by a central duplex of south-vergent Hercynian basement thrust sheets (the Axial Zone) flanked by north- and south-vergent fold and thrust belts to the north and south, respectively, and the associated foreland basins (e.g., Muñoz, 1992).

The PNOMP is part of the above-mentioned southern Pyrenean fold and thrust belt, formed by a set of imbricated thrust sheets (e.g., Seguret, 1972). The structural architecture of the PNOMP mainly responds to the presence of two major thrust sheets, the Gavarnie basement thrust sheet and the Monte Perdido cover thrust sheet (Seguret, 1972) (Fig. 1). The Gavarnie thrust appears at the northern part of the study area, where Paleozoic and upper Cretaceous rocks crop out (Fig. 1), whereas the Monte Perdido thrust sheet comprises Cretaceous to lower Eocene rocks with subhorizontal bedding around the Ordesa Valley (Fig. 1). Towards the south, these rocks are highly tilted and overlain by middle Eocene turbidites. The Monte Perdido thrust sheet has scarce internal deformation, which prevents local hydraulic connection between the different permeable levels (CHE, 1998). The upper Cretaceous and lower Paleocene–Eocene limestones, dolomites and calcarenites constitute the most important permeable outcropping materials and contain the most significant springs and water discharges in the study area. The main karst system is installed in the lower Paleocene–Eocene materials (CHE, 1998; Ríos-Aragüés, 2003).

From a hydrogeological point of view, the aquifer system is composed of two main units: (1) the upper unconfined aquifer, formed by Upper-Cretaceous (Cenomanian–Campanense) limestones of the Calizas del Estrecho and Marboré Formations, and (2) the lower and semi-confined aquifer, which is formed by Paleocene–Eocene (Danian–Lower Ilerdian) limestones and dolomites of the Gallinera and Salarons Formations. The upper and lower aquifer units are separated by the less permeable terrigenous facies of the Maestrichtian.

In the study area, the springs are spatially distributed between altitudes of 689 m and 2975 m a.s.l. Most of them are located in the contact between the limestones of the upper aquifer unit and the terrigenous facies of the Maestrichtian. Although the groundwater discharge is not continuously monitored in any spring of the PNOMP, the spring discharge rates show a high spatial heterogeneity, between 0.1 L/s and 100 L/s, all of which are permanent (Table 2). A seasonal flow rate variation has also been observed in the sampled springs, in agreement with the fast reaction to rainfall of spring discharge in such a developed karst system (Ríos-Aragüés, 2003; García-Ruiz et al., 2014).

Table 1 Atmospheric circulation pattern classification.

ACP type	Description
N/NW/W/SW	Northerly/northwesterly/westerly/southwesterly directional types
NE/E/SW/S	Northeasterly/easterly/southeasterly/southerly directional types
C	Cyclonic
UC	Unclassified/light flow-cyclonic
HYC	Hybrid-cyclonic
A	Anticyclonic
UA	Unclassified/light flow-anticyclonic
HYA	Hybrid-anticyclonic

Table 2 Groundwater sampling points (springs) and conducted field campaigns.

Code	Name	Discharge height (m a.s.l.)	Recharge height ^(a) (m a.s.l.)	ΔZ ^(a) (m)	Sector	Field campaigns			
						2007 ^(a)	2011 ^(a)	2012 ^(a)	2013 ^(a)
1	Arazas River	1130	3142	2012	Ordesa	Jul			
2	Fuen Plana Canal	1280	2815	1535	Ordesa	Jul			
3	Fuen Caño	1290	2978	1688	Ordesa	Jul			
4	As Fuens	1349	3025	1676	Ordesa		May, Jun, Jul, Aug, Sep, Oct, Nov, Dec	Mar, Apr	
5	Fuen Roya–Aguas Abajo	1348	3108	1760	Ordesa	Jul			
6	Fuen Roya–Surgencia	1358	3108	1750	Ordesa	Jul			
6A	Fuen Roya-1	1358	3319	1971	Ordesa				Sep

6B	Fuen Roya-2	1358	3091	1743	Ordesa				Sep
7	Fuen d ^a Arripas	1440	2923	1483	Ordesa	Jul			
8	Fuen as Gradas	1700	2915	1215	Ordesa	Jul			
9	Fuen Mochera	1807	3185	1435	Ordesa	Jul	Sep, Oct, Nov, Dec	Feb, Mar, Apr	
10	Fuen d ^a Abellá	1750	3197	1447	Ordesa	Jul			Sep
11	Fuen Cotatuero	1800	3067	1267	Ordesa	Jul			
12	Fuen De Soaso Torrente	1820	2739	919	Ordesa	Jul			
13	Fuen Carriata	1820	2763	943	Ordesa	Jul			
14	Fuen De Soaso	1830	2574	744	Ordesa	Jul			
15	Fuen Gallinero	1840	3041	1201	Ordesa	Jul			
16	Fuen Freda	1860	2913	1053	Ordesa	Jul			
17	Fuen de L'Abe	1920	2614	694	Ordesa	Jul			
18	Fuen Roldán	2136	2855	719	Ordesa		Aug, Sep, Oct, Nov	Mar	
19	Fuen de Goriz	2200	3062	862	Ordesa	Jul	May, Jun, Jul, Aug, Sep, Oct, Dec	Mar	
20	Fuen Fria	2340	3074	734	Ordesa	Jul			
21	Collado Millares	2420	3120	700	Ordesa	Jul			
22	Fuen dero Baño	689	2794	2105	Añisclo	Jul			Sep
23	Font Blanca	1710	3099	1389	Añisclo	Jul	May Jun, Jul, Sep, Oct, Nov	Mar	
24	Fuen dero Foratiello	1790	2670	880	Añisclo	Jul			
25	Fuen dero Furicón	2010	2753	743	Añisclo	Jul			
26	Fuen dero Esmoladera	2050	2725	675	Añisclo	Jul			
27	Fuen el Felcarral	1703	3076	1373	Pineta	Jul			
28	Fuen de la Bispeta	1930	2873	943	Pineta	Jul			
29	Fuen de Escuaín	1050	2500	1450	Escuaín	Jul	May, Jun, Jul, Aug, Sep, Oct, Nov	Mar, Apr	

^a Recharge level obtained from the local altitudinal line.

^b Difference between the recharge and discharge levels.

^c Major ions, $\delta^2\text{H}$, $\delta^{18}\text{O}$ and tritium.

^d Major ions, $\delta^2\text{H}$ and $\delta^{18}\text{O}$.

^e Major ions, $\delta^2\text{H}$, $\delta^{18}\text{O}$, $\delta^{34}\text{S}_{\text{SO}_4}$ and $\delta^{18}\text{O}_{\text{SO}_4}$.

According to the Köppen -Geiger climate classification (Peel et al, 2007), the PNOMP has a cold climate with a dry season, mild and cool summers, and significant altitudinal variations (AEMET/IM, 2011). The study area is covered by snow between October and June. At the Fanlo Góriz meteorological station (2200 m a.s.l.), located inside the PNOMP (see Fig. 1), the mean annual temperature is 4.9 °C, and the average precipitation is 1650 mm/yr. Precipitation presents two peaks in spring and autumn, at 220 and 185 mm/month, respectively, and two minima in winter and summer, at 80 and 105 mm/month, respectively (Fig. 2A).

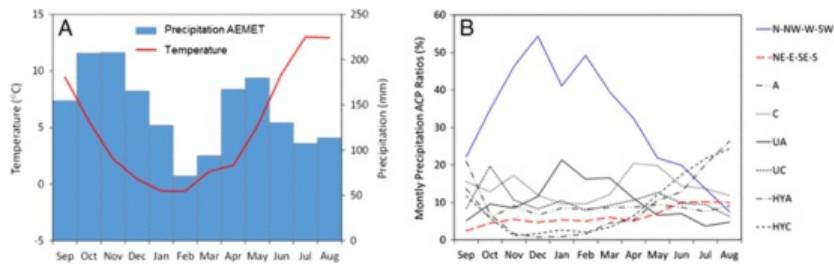


Fig. 2 (A) Average precipitation and temperature corresponding to the “Fanlo-Góriz” meteorological station (2200 m a.s.l.) for the period 1985–2005. The location of this station is marked with a red star in Fig. 1. (B) Ratio between the monthly ACP precipitation and the average monthly precipitation for the considered ACPs; blue bold lines and red dashed bold lines correspond to the directional ACPs blowing from the Atlantic and the Mediterranean side, respectively. [\(For interpretation of the references to colour in this figure legend, the reader is referred to the web version of this article.\)](#)

A relatively simple way to analyse the origin of rainfall in the PNOMP is to relate synoptic general atmospheric circulation patterns (ACPs) to local-scale precipitation (Goodess and Palutikof, 1998; Cortesi et al., 2013; Sapriza-Azuri et al., 2013, among others). This requires a method for classifying the ACPs into a discrete set of consistent ACP types. An automated version of the Lamb Weather Type classification scheme (Jenkinson and Collison, 1977; Jones et al., 1993) has been used, applied in accordance with Goodess and Palutikof (1998), that is based on the direction of surface wind and on its eddy characteristics in geostrophic units. For the study area, gridded values of mean sea level pressure at 16 points distributed across Spain are used, obtained from the gridded NCEP-NCAR reanalysis data set (Kalnay et al., 1996). The results allow the identification of eight ACP types, which are detailed in Table 1. The ACP scheme indicates that the higher rainfall amounts are associated with the directional type ACP (N/NW/W/SW), which brings moisture from the Atlantic during the autumn, winter and spring months (Fig. 2B). This result agrees with the W-E rainfall gradient reported by Benito Alonso (2006) for this region. Summer rainfall is mainly produced by the hybrid-cyclonic (HYC) and hybrid-anticyclonic (HYA) types, which are the typical conditions under which summer storms develop in mountain areas.

From an administrative perspective, following the European Water Framework Directive requirements (2000/60/CE; DMA), as transposed into the Spanish Water Law, the aquifer system of the PNOMP is included in the 09032 groundwater body named Sierra Tendeñera-Monte Perdido by the Ebro’s Hydrographic Confederation (CHE), which is the water authority.

3 Materials and methods

The sampling locations correspond to some of the most representative springs of the PNOMP (Table 2 and Fig. 1). Between July 2007 and September 2013, a number of groundwater sampling campaigns were performed (Table 2). The objective of these campaigns was threefold: (1) to explore the main geochemical signatures of the groundwater, (2) to examine possible seasonal rainfall isotopic variations, and (3) to measure the tritium content in the groundwater in selected springs (Fig. 1 and Table 3).

Table 3 Representative physical, chemical and isotopic data of groundwater in the study area during the field campaign conducted in 2007.

Sampling point code	Date	T ^(A)	pH ^(A)	EC ^(A)	DQO	HCO ₃	SO ₄	Cl	NO ₃	Na	K	Ca	Mg	SiO ₂	δ ² H	δ ¹⁸ O	d ^(B)	³ H ± σ
1	20/07/2007	10.5	8.15	197	0.5	83.0	22.0	1.0	1.0	0.0	0.0	26.0	8.0	1.3	74.9	10.7	10.7	
2	20/07/2007	10.9	8.29	302	0.5	162.0	12.0	1.0	1.0	0.0	0.0	37.0	15.0	4.6	68.0	9.5	8.3	6.08 ± 0.62
3	20/07/2007	9.6	7.98	388	0.6	163.0	47.0	1.0	1.0	0.0	0.0	38.0	24.0	4.5	71.2	10.2	10.0	5.72 ± 0.61
5	19/07/2007	10.5	7.89	930	0.5	103.0	380.0	3.0	0.0	2.0	0.0	136.0	40.0	5.7	75.7	11.0	11.9	4.89 ± 0.59
6	19/07/2007	9.3	7.75	405	0.5	102.0	100.0	2.0	1.0	0.0	0.0	52.0	17.0	3.1	75.7	11.0	11.9	4.89 ± 0.59
7	20/07/2007	11.6	8.11	306	0.7	149.0	26.0	1.0	0.0	0.0	0.0	40.0	14.0	3.2	69.7	10.0	10.2	4.87 ± 0.59
8	18/07/2007	7.5	8.13	304	0.5	133.0	48.0	1.0	0.0	0.0	0.0	34.0	20.0	4.8	69.3	10.0	10.7	4.93 ± 0.57
9	18/07/2007	7.0	7.94	92	0.5	61.0	13.0	1.0	0.0	0.0	0.0	14.0	8.0	0.3	75.9	10.9	10.9	4.98 ± 0.57
10	19/07/2007	11.4	8.04	361	0.5	95.0	86.0	1.0	1.0	0.0	0.0	35.0	22.0	5.4	75.7	11.0	11.9	4.89 ± 0.59
11	19/07/2007	10.0	8.11	299	0.5	108.0	40.0	2.0	1.0	0.0	0.0	33.0	14.0	4.0	72.7	10.5	11.5	5.46 ± 0.61

12	20/07/2007		8.33	244	0.6	124.0	16.0	1.0	0.0	0.0	0.0	37.0	8.0	2.6	64.6	9.5	11.3			
13	19/07/2007	16.4	8.13	221	0.6	111.0	19.0	1.0	0.0	0.0	0.0	33.0	8.0	2.6	66.6	9.4	8.5			
14	20/07/2007		6.87	434	2.5	232.0	8.0	1.0	0.0	0.0	0.0	69.0	9.0	1.5	61.2	8.9	10.1			
15	19/07/2007	12.1	8.29	274	0.6	106.0	33.0	2.0	0.0	0.0	0.0	34.0	11.0	3.0	71.9	10.5	11.7	4.55 ± 0.58		
16	20/07/2007	7.9	8.25	237	0.6	125.0	12.0	1.0	0.0	0.0	0.0	24.0	15.0	2.3	68.7	10.1	11.8			
18	20/07/2007	8.4	8.16	210	0.5	102.0	12.0	1.0	2.0	0.0	0.0	30.0	7.0	1.5	63.1	8.9	8.2	5.76 ± 0.62		
19	18/07/2007	11.5	8.19	120	0.5	57.0	13.0	1.0	1.0	0.0	0.0	18.0	5.0	0.5	72.9	10.5	10.7	4.82 ± 0.57		
20	18/07/2007		8.45	166	0.5	91.0	14.0	1.0	0.0	0.0	0.0	28.0	6.0	0.6	73.8	10.4	9.6	5.25 ± 0.58		
21	18/07/2007	8.7	8.58	140													74.6	10.6	10.3	
22	17/07/2007	26.0	7.05	3580	2.1	159.0	444.0	780.0	0.0	472.0	11.0	188.0	50.0	21.9	66.4	9.6	10.5	2.73 ± 0.52		
23	17/07/2007	9.2	8.40	123	0.6	54.0	12.0	1.0	0.0	0.0	0.0	16.0	5.0	0.4	74.0	10.6	10.4	3.81 ± 0.54		
24	17/07/2007	10.0	7.44	300	0.5	155.0	13.0	1.0	0.0	0.0	0.0	48.0	7.0	3.8	62.8	9.3	11.6	3.78 ± 0.54		
25	17/07/2007	7.1	7.70	368	0.8	174.0	13.0	2.0	1.0	0.0	0.0	52.0	9.0	2.4	63.5	9.7	14.3	4.97 ± 0.57		
26	17/07/2007	9.0	7.90	228	0.6	122.0	17.0	2.0	0.0	0.0	0.0	44.0	4.0	2.8	64.8	9.4	10.2	4.57 ± 0.56		
27	16/07/2007	14.9	7.72	237	0.5	108.0	19.0	1.0	1.0	0.0	0.0	33.0	8.0	2.0	72.9	10.5	11.4	1.00 ± 0.41		
28	16/07/2007	15.6	8.40	139	0.6	68.0	14.0	1.0	1.0	0.0	0.0	14.0	10.0	0.8	69.0	9.8	9.1	2.17 ± 0.45		
29	26/07/2007	14.1	8.50	220	0.6	88.0	19.0	1.0	1.0	0.0	0.0	31.0	5.0	1.8	60.9	8.5	6.8	4.97 ± 0.55		

Units: T in °C, EC in µS/cm, hydrochemical ion concentration in (mg/L), DQO in (mg/L), δ²H, δ¹⁸O and d in ‰, and tritium content in UT.

^a Field parameters.

^b Deuterium excess (d = δ²H - 8δ¹⁸O - δ²H‰).

Sampling groundwater in the PNOMP is not easy because the rough topography of the study zone, and the very difficult access and material transportation to some points hampered the operations, which had to be simplified. Thus, none of the groundwater samples were filtered or acidified in the field. In all cases, however, electrical conductivity (EC), pH and temperature (T) were measured in situ, and all of the groundwater samples were stored in polyethylene bottles at 4 °C until analysis. A total of 106 groundwater samples were obtained during the different field sampling campaigns.

In the field campaign conducted in July 2007, 25 springs were sampled between 690 m and 2400 m a.s.l., and a further sample was taken from the Arazas River (site 1; see location in Fig. 1) at 1130 m a.s.l. All groundwater samples of this first campaign were analysed for δ¹⁸O, δ²H composition and tritium content (Table 3). The chemical analyses were carried out at the IGME Water Laboratory (Madrid) and the isotope analyses at the CETA-CEDEX Laboratory (Madrid).

In the laboratory, pH and EC measurements were made by electrometry (pH_imeter HM model 781 and CRISON model MICRO CM2201, respectively); COD-oxidability was volumetrically determined via boiling in an acid medium and evaluation with potassium permanganate; bicarbonate, ammonia, silica, calcium and magnesium were determined by molecular absorption in continuous flow using an ALLIANCE autoanalyser, model INTEGRAL PLUS; chloride, sulphate and nitrate were determined by ionic chromatography; sodium and potassium were determined by atomic absorption spectroscopy with a VARIAN equipment model SPECTRA AA 220; and carbonate ions were determined by titration. The chemical components measured in all samples from all campaigns were the same: HCO₃⁻, Ca²⁺, Mg²⁺, Na⁺, K⁺, Cl⁻, SO₄²⁻, NO₃⁻, SiO₂.

The δ¹⁸O and δ²H were measured by SMS (small mass spectrometer), a Delta Plus Advantage model by Finnigan MAT. The isotopic composition of oxygen was determined through the water-CO₂ equilibration technique and that of hydrogen through the water-H₂ equilibration technique using a platinum catalyst. The reproducibility calculated from standards systematically interspersed in the analytical batches is ± 0.2‰ for δ¹⁸O and ± 1.5‰ for δ²H. The laboratory standards were regularly calibrated according to international standards (Vienna Standard Mean Ocean Water, VSMOW). Tritium analyses were carried out by means of a Quantulus 1220 liquid scintillation spectrometer, with a measurement error between ± 0.33 and ± 0.42 TU.

Between May 2011 and April 2012, following a monthly schedule, groundwater samples were obtained from six springs (Table 2). In this case, the groundwater samples were only analysed for $\delta^{18}\text{O}$ and $\delta^2\text{H}$ (see Table 4).

Finally, in September 2013, groundwater samples were obtained from four springs (see Table 2). The isotopic analyses included $\delta^{18}\text{O}$, $\delta^2\text{H}$, $\delta^{34}\text{S}_{\text{SO}_4}$, and $\delta^{18}\text{O}_{\text{SO}_4}$ (Table 5). (See Table 4.)

Table 4 Representative physical, chemical and isotopic data of groundwater in the study area during the field campaigns conducted in 2011 and 2012.

Sampling point code	Date	T ^(a)	pH ^(a)	EC ^(a)	HCO ₃	SO ₄	Cl	NO ₃	F	Na	K	Ca	Mg	SiO ₂	TA ^(b)	TDS ^(c)	$\delta^2\text{H}$	$\delta^{18}\text{O}$	d ^(d)
19	24/05/2011	6.2	8.08	182	132.0	0.6	0.9	0.2	0.0	1.1	0.0	45.6	1.4	132.0	132.0	140	73.3	10.8	12.9
9	24/05/2011	8.4	8.48	148	107.2	1.2	0.1	0.3	0.0	0.3	0.0	34.7	2.5	111.3	111.3	104	76.1	10.6	9.1
4	24/05/2011	8.0	8.05	298	165.0	29.5	1.1	0.6	0.0	1.1	0.0	51.3	15.4	165.0	165.0	252	72.2	10.0	7.5
23	25/05/2011	8.2	8.45	113	84.8	1.2	0.2	1.0	0.0	0.1	0.0	24.1	2.3	86.4	86.4	84	74.2	10.8	11.8
29	26/05/2011	9.2	8.19	88	101.7	2.7	0.1	0.8	0.0	0.1	0.0	31.2	2.2	101.7	101.7	96	71.0	10.3	11.9
19	30/06/2011	10.6	8.16	210	73.5	0.9	0.1	0.5	0.0	0.2	0.0	35.6	1.8	73.5	73.5	128	69.5	10.6	15.2
9	30/06/2011	13.9	8.89	140	52.6	1.3	0.2	0.4	0.0	0.4	0.0	22.8	2.6	54.5	54.5	88	72.4	10.9	14.4
4	29/06/2011	9.5	7.93	380	88.5	30.0	0.8	0.6	0.0	1.1	0.0	44.4	14.3	88.5	88.5	236	71.3	10.3	10.9
23	29/06/2011	10.3	8.73	117	43.6	1.5	0.3	0.7	0.0	0.1	0.0	16.4	1.4	43.6	43.6	80	68.0	10.2	13.3
29	29/06/2011	11.3	8.41	222	65.8	7.5	0.2	0.9	0.0	0.2	0.0	28.9	4.0	65.8	65.8	132	65.3	9.5	10.8
19	30/07/2011	12.0	8.42	180	59.7	1.3	0.1	0.4	0.0	0.3	0.0	37.4	1.8	61.4	61.4	124	69.1	9.5	7.2
9	30/07/2011	12.9	8.19	170	62.9	2.2	0.1	0.4	0.0	0.4	0.0	38.3	4.6	66.2	66.2	136	70.6	9.6	5.9
4	30/07/2011	10.7	7.89	290	87.7	37.9	0.7	0.6	0.0	1.1	0.0	52.8	15.6	87.7	87.7	260	71.3	9.9	7.9
23	31/07/2011	11.3	8.20	120	47.6	2.2	0.1	0.6	0.0	0.7	0.0	24.8	2.3	47.6	47.6	120	72.3	9.9	6.5
29	31/07/2011	11.6	8.41	230	64.6	14.0	0.2	0.9	0.0	0.5	0.0	43.4	7.2	68.8	68.8	176	66.3	9.2	7.1
19	25/08/2011	10.7	7.94	230	81.4	2.0	0.3	1.5	0.0	0.3	0.0	41.4	2.3	81.4	81.4	144	52.2	8.3	14.3
9	24/08/2011	6.5	8.56	150	66.7	4.4	0.2	1.2	0.0	0.3	0.0	26.9	5.0	66.7	66.7	108	67.2	9.9	12.2
4	24/08/2011	10.0	8.36	400	107.3	54.4	0.9	0.8	0.0	1.0	0.0	51.7	16.0	107.3	107.3	244	70.8	10.9	16.4
29	26/08/2011	11.4	8.28	180	89.5	6.3	0.3	1.1	0.0	0.3	0.0	39.3	3.8	92.4	92.4	148	55.6	8.7	13.8
18	25/08/2011	8.9	8.05	150	81.2	1.4	0.3	2.0	0.0	0.2	0.0	36.4	0.9	81.2	81.2	124	45.3	7.4	13.5
19	30/09/2011	10.8	8.02	365	203.1	1.3	0.3	0.6	0.0	0.2	0.0	43.5	2.4	203.1	203.1	188	55.1	8.4	11.9
9	30/09/2011	5.8	7.88	194	114.1	5.1	0.2	1.5	0.0	0.0	0.0	24.5	4.9	114.1	114.1	112	66.0	10.2	15.4
4	30/09/2011	8.1	7.83	356	142.0	46.1	0.3	0.7	0.0	0.1	0.0	40.2	12.6	142.0	142.0	216	68.8	10.5	14.9
23	29/09/2011	12.6	8.34	100	107.4	3.4	0.2	1.2	0.0	0.0	0.0	24.2	3.1	113.8	113.8	104	54.8	8.5	13.5
29	29/09/2011	10.9	8.28	100	132.3	12.7	0.2	1.0	0.0	0.1	0.0	29.4	5.8	136.4	136.4	116	59.2	9.1	13.3
18	30/09/2011	10.3	8.05	273	156.0	2.5	1.4	4.1	0.0	0.9	2.0	44.1	2.6	156.0	156.0	224	52.3	8.3	13.8
19	26/10/2011	8.7	8.34	147	146.2	1.5	0.5	1.0	0.0	0.2	0.0	45.4	1.9	146.2	146.2	116	61.2	9.6	15.5
9	26/10/2011	4.9	5.60	210	124.3	3.3	0.5	1.1	0.0	0.3	0.0	33.2	3.9	124.3	124.3	116	68.6	10.4	14.6

4	26/10/2011	6.9	5.20	390	139.8	54.6	0.3	0.7	0.0	0.5	0.0	50.1	14.8	139.8	139.8	248		68.5		10.3	13.7
23	29/10/2011	7.9		187	110.9	1.5	0.3	1.0	0.0	0.2	0.0	28.0	2.0	114.2	114.2	72		68.6		10.7	17.4
29	29/10/2011	9.5		209	125.4	2.4	0.3	1.0	0.0	0.2	0.0	35.9	2.9	125.4	125.4	96		65.7		10.4	17.3
18	26/10/2011	8.3	5.20	160	125.0	1.2	1.1	1.4	0.0	0.7	0.5	39.4	0.8	125.0	125.0	116		61.0		9.2	12.7
19	29/11/2011	6.7		160	149.4	0.6	0.2	0.2	0.0	0.0	0.0	37.1	1.4	153.0	153.0	164		74.1		11.1	14.5
9	29/11/2011	5.4		140	115.6	2.6	0.2	1.0	0.0	0.0	0.0	26.5	3.8	115.6	115.6	108		76.1		11.5	15.7
4	29/11/2011	7.4		270	137.9	31.5	0.4	0.9	0.1	0.4	0.0	36.3	10.3	137.9	137.9	200		68.1		10.2	13.3
23	30/11/2011	3.7		176	115.8	2.4	0.2	0.8	0.0	0.0	0.0	25.5	2.4	118.2	118.2	116		68.6		10.5	15.7
29	30/11/2011	7.4		220	126.7	8.0	0.2	0.9	0.0	0.0	0.0	30.0	4.5	131.1	131.1	144		67.3		10.2	14.2
18	29/11/2011	9.0		120	118.0	1.0	0.4	3.5	0.0	0.4	0.0	31.6	1.1	121.3	121.3	124		81.5		12.1	15.1
9	23/12/2011	5.6	8.30	170	122.0	4.5	0.1	1.0	0.0	0.0	0.0	30.8	5.6	122.0	122.0	108		79.1		11.6	13.6
4	23/12/2011	8.5	7.85	370	144.7	40.4	0.3	0.7	0.0	0.0	0.0	46.7	12.1	144.7	144.7	200		69.8		10.6	15.2
9	28/02/2012	8.4	6.40	190	112.6	5.0	0.2	1.2	0.0	0.1	0.0	29.1	5.3	112.6	112.6	112		74.1		11.5	17.5
19	28/03/2012	8.4	6.40	200	133.6	1.1	0.2	0.5	0.0	0.0	0.0	41.4	1.1	133.6	133.6	136		73.8		11.5	18.0
9	28/03/2012	8.5	6.40	160	108.0	2.2	0.2	1.1	0.0	0.0	0.0	33.0	3.5	108.0	108.0	108		78.2		11.7	15.0
4	28/03/2012	8.1	6.40	350	126.2	53.6	0.4	0.8	0.0	0.0	0.0	42.4	12.5	126.2	126.2	244		70.5		10.7	14.8
23	27/03/2012	8.5	6.40	140	101.6	2.0	0.3	1.5	0.0	0.0	0.0	28.1	2.0	101.6	101.6	104		69.2		10.7	16.7
29	28/03/2012				101.4	4.8	0.3	1.5	0.0	0.0	0.0	30.9	2.9	101.4	101.4	120		64.5		9.9	15.0
18	28/03/2012	8.6	6.40	110	94.3	1.2	0.4	2.0	0.0	0.3	0.0	31.7	0.7	94.3	94.3	108		73.8		10.9	13.0
9	24/04/2012				114.7	3.1	0.2	1.1	0.0	0.9	0.0	33.4	4.4	115.8	115.8	108		74.6		11.0	13.6
4	24/04/2012				124.0	36.8	0.3	0.8	0.0	0.3	0.0	47.5	13.6	124.0	124.0	204		68.7		10.1	12.4
29	24/04/2012				125.3	4.9	0.2	0.7	0.0	0.4	0.0	38.8	4.6	131.6	131.6	128		64.3		9.6	12.6

Units: T in °C, EC in µS/cm, hydrochemical ion concentration in (mg/L), TA (mg/L), TDS in %, and isotope content in ‰.

^a Field parameters.

^b Total alkalinity.

^c Total dissolved solids.

^d Deuterium excess ($d = \delta^{18}O - \delta^2H$ ‰).

Table 5 Representative physical, chemical and isotopic data for groundwater in the study area for the field campaign conducted in 2013.

Sampling point code	Date	T ^(a)	pH ^(a)	EC ^(a)	HCO ₃	SO ₄	Cl	NO ₃	Na	K	Ca	Mg	SiO ₂	δ ² H	δ ¹⁸ O	d ^(b)	δ ¹⁸ O _{SO₄}	δ ³⁴ S _{SO₄}			
6A	15/09/2013	9.2	7.2	2190	114.0	1340.8	2.5	0.1	7.3	0.7	424.0	89.0	11.7		74.9		11.8		13.8	17.3	18.3
6B	15/09/2013	9.7	7.5	707	139.0	245.8	0.8	0.4	1.9	0.2	102.0	32.0	4.1		72.4		10.7		13.2	16.2	16.9
10	15/09/2013	7.9	7.8	350	99.0	85.6	0.4	0.2	1.9	0.2	39.0	18.0	4.5		75.0		11.7		13.5	14.0	13.7

22	15/09/2013	24.8	7.2	3150	209.0	491.5	639.1	0.2	510.0	16.3	166.0	32.0	17.8	64.3	9.6	12.6	15.0	17.7
Rainfall ^c	30/09/2013				5.0	1.7	0.31	1.14	0.24	0.1	1.0	1.0	0.0	34.8	6.6	18.0		

Units: T in °C, EC in $\mu\text{S}/\text{cm}$, hydrochemical ion concentration in (mg/L) and isotope content in ‰.

^a Field parameters.

^b Deuterium excess ($d = \delta^2\text{H} - 8\delta^{18}\text{O}$ ‰).

^c Monthly accumulated rainfall at the Góriz Meteorological station.

The groundwater chemical analyses of the field campaigns between May 2011 and September 2013 were performed at the laboratories of the Pyrenean Institute of Ecology (CSIC) and the $\delta^{18}\text{O}$ and $\delta^2\text{H}$ measurements at the IACT-CSIC (Granada). Standard techniques were applied for measuring the total dissolved solids and the total suspended solids (gravimetric method, APHA, 1989, 2540 C & D), the particulate organic matter (gravimetric method, APHA, 1989, 2540 E) and the soluble reactive phosphorus (colorimetry, APHA, 1989, 4500 PE). The alkalinity was measured using a Metrohm 798 MPT Titrimo automated titrator (APHA, 1989, 2320 B). Ions were analysed using an ionic chromatograph (Metrohm 861 Advanced compact IC), fitted with a 20-mL sampling loop, a Metrosep A Sup 2 polystyrene-divinylbenzene polymer column with chemical suppressor for anions detection, Metrosep C 2-250 silica gel with carboxyl groups for cation determination and a conductivity detector (APHA, 1989, 4110 B). Total organic carbon (TOC) and total nitrogen (TN) were measured with a Multi-N/C 3100 analyser, Analytik Jena®, using the Multi-Channel-Non Dispersive Infrared Detector (MC-NDIR) for TOC (APHA, 1989, 5310 B) and chemiluminescence for TN. The $\delta^{18}\text{O}$ and $\delta^2\text{H}$ were analysed with a Finnigan Delta Plus XL mass spectrometer. The measurement errors for $\delta^{18}\text{O}$ and $\delta^2\text{H}$ are ± 0.1 and ± 1.5 ‰, respectively. The results are given relative to the V-SMOW standard.

The sulphate isotopic analyses ($\delta^{34}\text{S}_{\text{SO}_4}$ and $\delta^{18}\text{O}_{\text{SO}_4}$) were only performed in samples with a significant dissolved sulphate content sampled in the September 2013 field campaign. The samples were prepared in the Applied Mineralogy and Environment Research Group laboratory and were analysed at the "Centres de Tècniques Científiques" of the Universitat de Barcelona. For the isotopic analysis of sulphate, dissolved sulphate was precipitated as BaSO_4 by adding $\text{BaCl}_2 \cdot 2\text{H}_2\text{O}$ after acidifying the sample with HCl and boiling it to prevent BaCO_3 precipitation following standard methods (e.g., Dogramaci et al., 2001). The $\delta^{34}\text{S}$ was measured in a Carlo Erba Elemental Analyzer (EA) coupled in continuous flow to a Finnigan Delta C IRMS. The $\delta^{18}\text{O}$ was determined in duplicate with a ThermoQuest high temperature conversion analyser (TC/EA) unit with a Finnigan Matt Delta C IRMS. Isotope ratios were calculated using three international samples and one internal laboratory reference sample. The results are given relative to the V-SMOW for $\delta^{18}\text{O}$ and V-CDT for $\delta^{34}\text{S}$. The precision (2σ) of the samples calculated from international and internal standards systematically interspersed in the analytical batches was ± 0.2 ‰ for $\delta^{34}\text{S}$ and ± 0.5 ‰ for $\delta^{18}\text{O}$.

4 Results

4.1 Hydrogeochemistry

In the field campaign conducted in 2007, which was the most extensive, the measured EC values ranged between 102 and 3673 $\mu\text{S}/\text{cm}$. Nevertheless, in 92% of the springs, the measured EC was lower than 400 $\mu\text{S}/\text{cm}$, which is the average EC value obtained in this field campaign. The pH ranges between 6.8 and 8.6. The sampled groundwaters have a calcium-bicarbonate or calcium-magnesium-bicarbonate composition (Fig. 3), which is in agreement with the carbonate nature of the main permeable materials (upper Cretaceous and lower Paleocene-Eocene limestones, dolomites and calcarenites) found in the PNOMP. The sampled groundwater show two additional hydrogeochemical facies: (A) calcium-sulphate composition in the Fuen I Abellá (site 10), Fuen Roya Aguas Abajo (site 5), and Fuen Roya Surgencia (site 6) springs, which are located in nearby sectors and suggest a possible connection and a dominant anhydrite and/or gypsum dissolution process; and (B) sodium-chloride-sulphate composition in the Fuen dero Baño spring (site 22), with an EC of 3600 $\mu\text{S}/\text{cm}$ and an in-situ T of 26 °C that clearly contrasts with the average EC of 250 $\mu\text{S}/\text{cm}$ and T of 10.5 °C measured in other springs in the PNOMP. The Fuen dero Baño spring (site 22) is located at the southernmost end of the PNOMP, relatively far from the other sampled springs, at the lowest altitude sector (Fig. 1). Therefore, its location could account for these differences with respect to the other sampling points located northward.

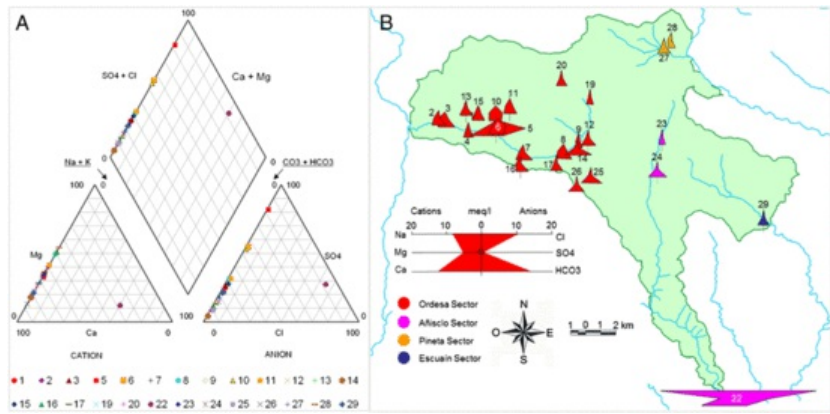


Fig. 3 Piper (A) and modified Stiff diagrams (B) for the July 2007 field campaign. The site numbers correspond to those of Table 1.

The EC is positively correlated with the bicarbonate, and calcium content exists (Fig. 4A). Moreover, with $r_{HCO_3}/r_{Ca} \sim 1$ and $r_{Mg}/r_{Ca} < 1$ (Fig. 4B and C, respectively), a dominant calcite dissolution process can be assumed (r means the concentrations are expressed in meq/L).

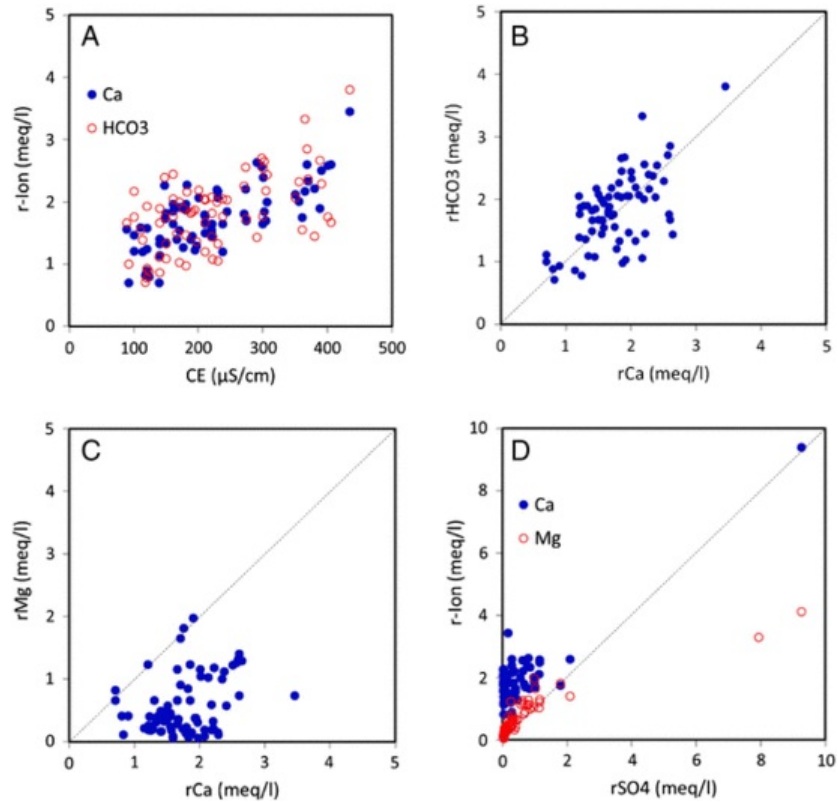


Fig. 4 Relationships between (A) EC and both r_{HCO_3} and r_{Ca} ; (B) r_{Ca} and r_{HCO_3} ; (C) r_{Ca} and r_{Mg} ; (D) r_{SO_4} and both r_{Mg} and r_{Ca} . Field campaigns 2007 and 2011.

The rMg/rSO_4 and rCa/rSO_4 ratios are plotted in Fig. 4D. The rCa/rSO_4 ratio is larger or close to 1 in most of the sampled springs. Nevertheless, in the Fuen Roya springs (sites 5 and 6) and the Fuen dero Baño spring (site 22), the ratio is clearly lower than 1 (i.e., 0.42, 0.67 and 0.45, respectively) due to the higher sulphate content. Additionally, the rCa/rSO_4 ratio is close to 1 in the Fuen Abellá (site 10) and Fuen dero Baño (site 22) springs (i.e., 0.98 and 1.02, respectively).

In the Ordesa Valley sector (see Fig. 5), where it is possible to analyse the hydrochemical variations of groundwater composition in a spatially detailed way, the relation between the rCa and $rHCO_3$ with respect to EC is better defined by linear relationships (Fig. 5). Additionally, in this sector, the rMg/rCa and rCa/rSO_4 ratios are directly and inversely correlated with the magnesium contents, respectively (Fig. 6).

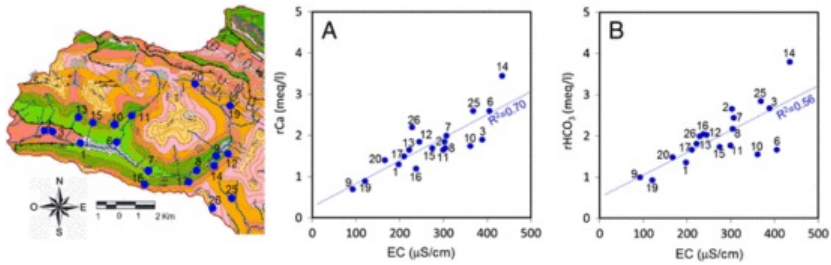


Fig. 5 Relationships between (A) EC and rCa and (B) EC and $rHCO_3$ obtained from the Ordesa Valley sector during the 2007 field campaign. The numbers correspond to those of Table 1.

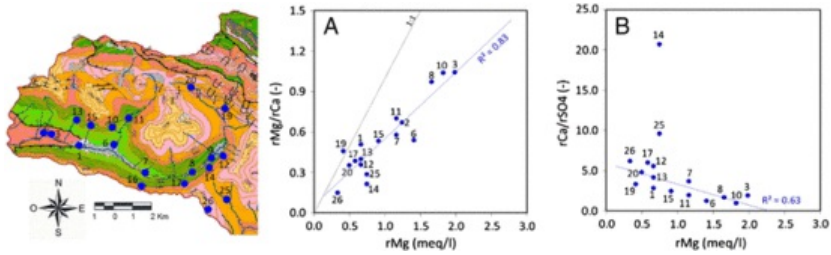


Fig. 6 Relationships between (A) rMg and rMg/rCa and (B) rMg and rCa/rSO_4 obtained from the Ordesa Valley sector during the 2007 field campaign. The numbers correspond to those of Table 1.

4.2 Stable isotopes

The groundwater samples obtained in the PNOMP present an isotopic composition ranging between -7.4‰ and -12.3‰ for $\delta^{18}O$ and between -45.3‰ and -81.5‰ for δ^2H , with coefficients of variation of the sets of 0.091 for $\delta^{18}O$ and 0.093 for δ^2H .

The $\delta^{18}O$ composition shows a linear dependence (Fig. 7) with altitude in the highest springs (i.e., above 1900 m). An apparent vertical isotopic gradient of -0.32‰ $\delta^{18}O/100$ m is obtained, which is comparable to the vertical gradients reported by Arce et al. (2001) and Iribar and Antigüedad (1996) in other Pyrenean sectors westward.

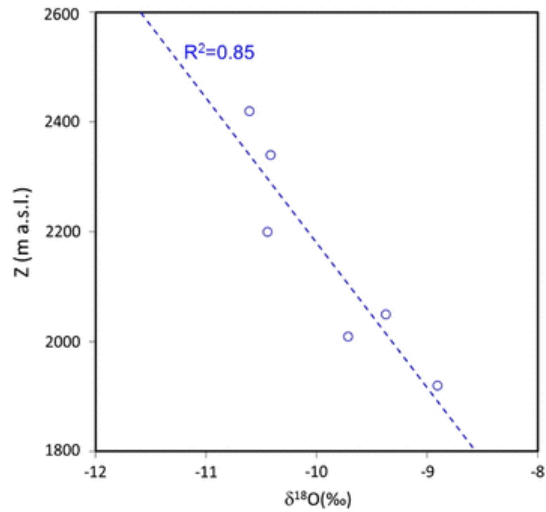


Fig. 7 Relationship between $\delta^{18}\text{O}$ and altitude for samples taken in the springs located above 1900 m during the 2007 field campaign. The apparent altitudinal isotopic gradient is $-0.32\text{‰ } \delta^{18}\text{O}/100 \text{ m}$.

Fig. 8 shows the seasonal averages of $\delta^{18}\text{O}$ and $\delta^2\text{H}$ in springs for the PNOMP and in three additional rainfall sampling stations located on the Pyrenean axis: Santander (IAEA-GNIP), at sea level and under Atlantic influence; (2) Estopiñán (Pérez, 2013), 30 km away towards the SE, at 750 m a.s.l.; and (3) Barcelona (IAEA-GNIP), at sea level and under Mediterranean influence. The seasonally averaged isotopic composition in the PNOMP is lighter than those observed in the other precipitation sampling stations (i.e., Estopiñán, Santander and Barcelona). This is due to the higher altitude and lower temperature in the PNOMP. Although the geographical positions of the PNOMP and Estopiñán are equivalent from a synoptic scale viewpoint (Hannah and McGregor, 1997), the seasonally averaged isotopic groundwater compositions of springs in the PNOMP show a deuterium excess ($d = \delta^2\text{H} - 8\delta^{18}\text{O}$) not observed in Estopiñán. Deuterium excesses coincide with the seasonal presence of snow covering nearly the entire PNOMP between October and June.

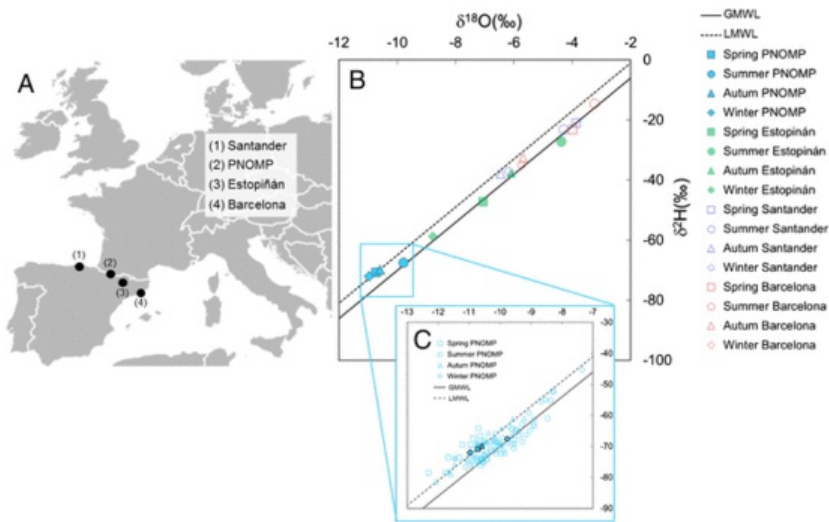


Fig. 8 (A) Geographic location of the PNOMP and the precipitation isotope sampling stations of Santander, Estopiñán and Barcelona and (B) $\delta^{18}\text{O}$ and $\delta^2\text{H}$ seasonal averages. The solid line and densely dashed line are the global mean meteoric water line (GMWL) and the local mean meteoric water line (LMWL) of slope $m = 8$ and deuterium excess of $+10$ and $+15\text{‰}$, respectively. (C) Measured and seasonally averaged values of $\delta^{18}\text{O}$ and $\delta^2\text{H}$ (open and solid symbols, respectively) in the PNOMP.

All sampling spring points show that the $\delta^{18}\text{O}$ and $\delta^2\text{H}$ contents follow a sinusoidal trend (Fig. 9), with heavier isotopic compositions in summer and lighter compositions in autumn and winter, in agreement with the observed relationship between the

isotopic fractionation and temperature (Clark and Fritz, 1997). Moreover, springs located at higher altitudes (Fig. 9-A) present larger annual $\delta^{18}\text{O}$ and $\delta^2\text{H}$ oscillations than springs located at lower altitudes (Fig. 9-B). A sinusoidal function was automatically calculated to fit the measured isotopic time series of the $\delta^{18}\text{O}$ and $\delta^2\text{H}$ oscillations in spring water, using a minimum square criterion (Press et al., 1992). The sinusoidal function is given by $\delta C = \mu + A \cdot \sin(\omega t + \phi)$, where δC is the isotopic composition, μ is the average isotopic composition, t is time, A is the amplitude, ϕ is the angular shift and ω is the angular frequency. The amplitude A and the angular shift ϕ are parameters to be estimated.

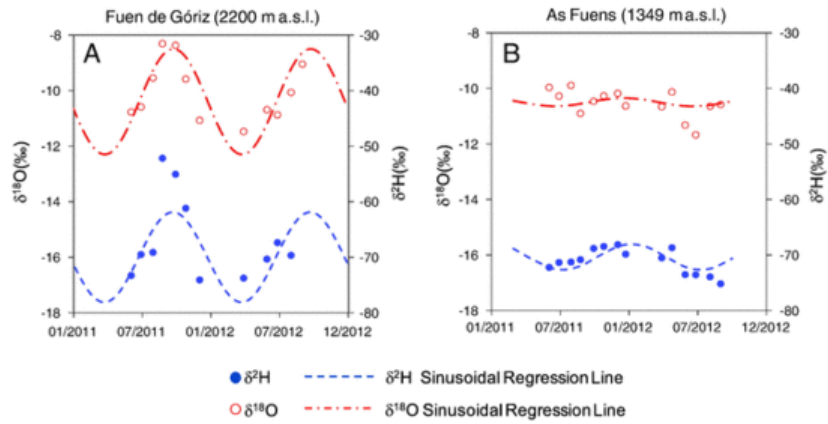


Fig. 9 Temporal evolution of the $\delta^{18}\text{O}$, $\delta^2\text{H}$ concentrations during the 2011–2012 field campaign at Fuen de Góriz (A) and As Fuens (B) springs.

The estimated parameters show a linear relationship with the difference ΔZ between the assumed recharge and the discharge altitudes of the sampled springs (Fig. 10). This reveals that the isotopic input signal is delayed and progressively buffered as ΔZ increases.

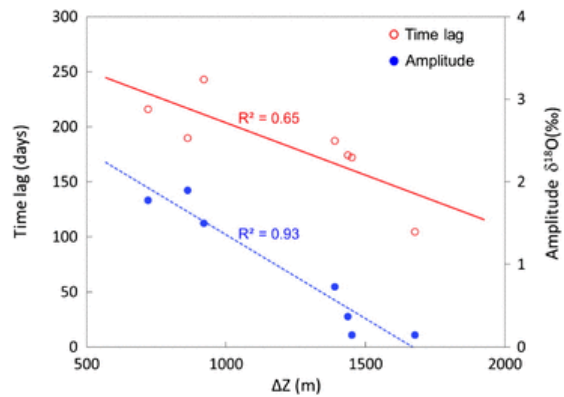


Fig. 10 Time lag and $\delta^{18}\text{O}$ amplitude versus altitude difference ΔZ between recharge area and discharge site of the 2011–2012 field campaign. This time lag depends on the signal time lag and depth, so it decreases with increasing depth (Jódar et al., 2014).

For the isotopic analysis of $\delta^{34}\text{S}_{\text{SO}_4}$ and $\delta^{18}\text{O}_{\text{SO}_4}$, it was necessary to select springs with a significant dissolved sulphate content. During the last field campaign performed in September 2013, four springs were sampled (Table 5). The $\delta^{34}\text{S}_{\text{SO}_4}$ ranged from +13.7 to +18.3‰ and the $\delta^{18}\text{O}_{\text{SO}_4}$ from +14 to +17.3‰. The sample from the L^lAbellá spring (site 10) presents lighter isotope compositions than those obtained in the other three sampled springs (sites 6A, 6B and 22) (Fig. 11).

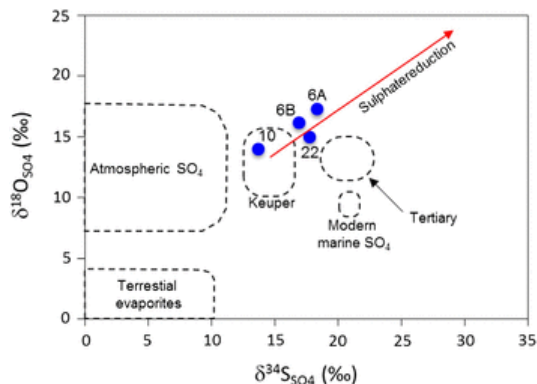


Fig. 11 $\delta^{18}\text{O}_{\text{SO}_4}$ vs $\delta^{34}\text{S}_{\text{SO}_4}$ for the analysed groundwater samples (modified from Clark and Fritz, 1997). The numbers correspond to those of Table 1.

4.3 Tritium

The tritium content in the groundwater was analysed only in water samples collected during the July/2007 field campaign. It ranges between 6.1 ± 0.6 TU and 4.6 ± 0.6 TU, with a coefficient of variation of the set of 0.093.

Although measurements of tritium in rainfall are not available at the PNOMP, the tritium content in rainfall is regularly measured at the REVIP (Spanish Vigilance Network of Precipitation Isotopes) stations (Fig. 12). The results show small variations in tritium concentrations during the last 15 years, with no trend (Díaz-Teijeiro et al., 2009).

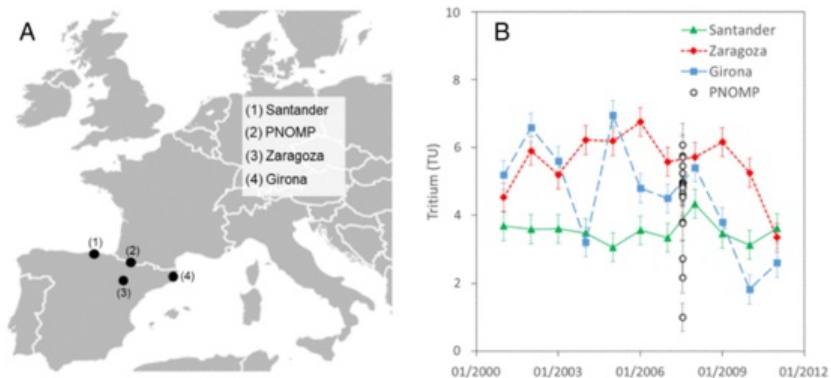


Fig. 12 (A) Geographic position of the PNOMP and the closest precipitation sampling station for tritium (Santander, Zaragoza and Girona) REVIP stations and (B) time series of tritium concentration measured at the PNOMP and selected REVIP stations. Note that the late tritium decrease in the Mediterranean stations is not produced at Santander station, which is in the path of incoming rainfall to the PNOMP.

The tritium concentration in rainfall from the stations closest to the study area is close to those measured in the sampled springs, indicating short transit times of recharge water through the aquifer.

The springs of Fuen el Felcarral (site 27) and Fuen la Bispeta (site 28) in the Pineta sector and of Fuen dero Baño (site 22) in the Añisclo sector, showed the lowest tritium contents, with measured activities of 1.00 ± 0.41 TU, 2.17 ± 0.45 TU and 2.73 ± 0.52 TU, respectively.

5 Discussion

In the Ordesa valley (Fig. 1), where most of the sampling was conducted, the groundwater EC and the major ion (i.e., magnesium, calcium and bicarbonate) contents are well correlated (R^2 values of 0.73, 0.70 and 0.56, respectively). These ions together with the $r\text{Mg}/r\text{Ca}$ ratio (r = concentration in meq/L) in the groundwater decrease with altitude. Large differences between the assumed recharge and the discharge altitudes of the different springs play a major role in the hydrogeochemical evolution of this karst system, particularly in the magnesium content and the $r\text{Ca}/r\text{SO}_4$ and $r\text{Ca}/r\text{SO}_4$ ratios (Fig. 13). The magnesium content of the groundwater increases with increasing altitude difference between recharge and discharge zones (Fig. 13-A and -B), while the calcium content decreases as the altitude difference increases (Fig. 13-B and -C).

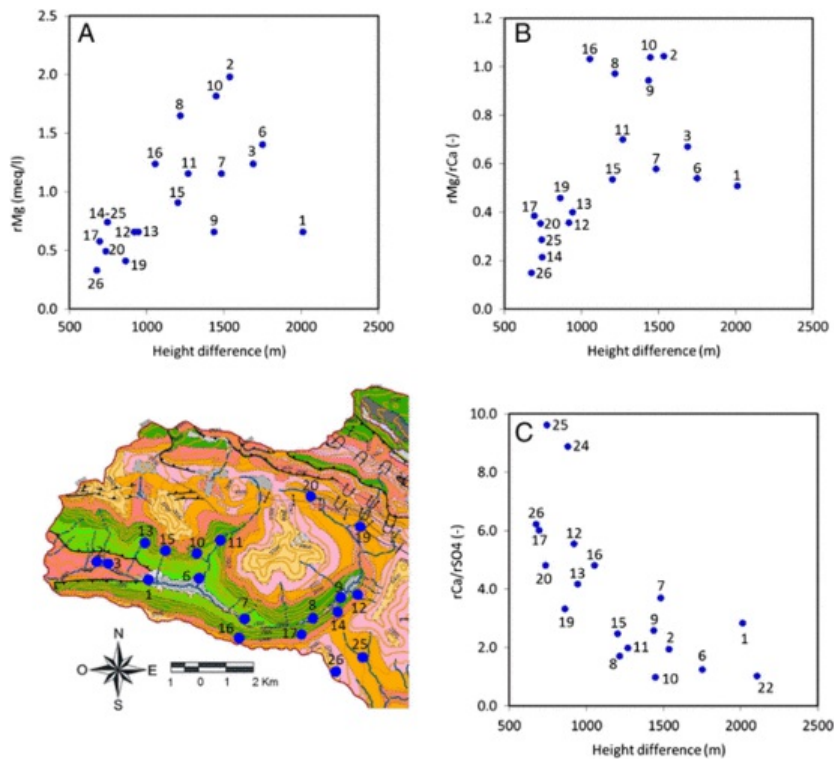


Fig. 13 Variation of the relationships rMg , rMg/rCa and rCa/rSO_4 regarding the altitude difference in the geographical environment of the Ordesa Valley during the 2007 field campaign. The numbers correspond to those of Table 1.

Rainfall originating at the Atlantic Ocean is the main source of aquifer recharge in the PNOMP. The averaged summer $\delta^{18}O$ and δ^2H isotopic composition in groundwater is close to the World Meteoric Water Line (GMWL), but the averaged isotopic composition for the other three seasons shows a deuterium excess greater than 10‰. This is interpreted as resulting from the presence of snow covering the recharge area during the autumn, winter and spring months. Snow sublimation is an important mass loss mechanism in high mountain systems that, in extreme cases, can exceed 3 mm/day (Vuille, 1996). Sublimation is produced in the upper layers of the snow cover and it reaches the maximum during the hours of highest sun irradiation in warm hours, provided the snow cover persists. As a result of diurnal sublimation, the remaining snow becomes isotopically enriched and has a lower deuterium excess, while the sublimated water vapour becomes lighter and has a higher deuterium excess. This vapour, mostly produced in the lower areas, mixes with vapour coming from neighbouring zones such as the Atlantic coast. The resulting vapour increases its atmospheric deuterium excess at the local scale. The low night temperatures at high elevation cause the atmospheric water vapour to condense on the snow surface, and as a result, the snow cover there increases its deuterium excess (Stichler et al, 2001; Froehlich et al., 2008). This diurnal snow sublimation and nocturnal condensation cycle could explain why the recharge due to high altitude snow melt in autumn, winter and spring has an increased deuterium excess in the PNOMP.

Although the possible influences of changing recharge isotopic composition along the slope in spring water composition (see Custodio, 2010) are not considered, a linear relationship between the groundwater $\delta^{18}O$ composition and the altitude of the highest springs (i.e., above 1900 m) is observed in the PNOMP. A vertical isotopic gradient of $-0.31\text{‰ } \delta^{18}O/100\text{ m}$ is obtained, which is coherent with the gradients reported by Arce et al. (2001) and Iribar and Antigüedad (1996) for the western Pyrenees. The altitude differences for all sampling points, therefore, can be estimated by taking the above altitudinal $\delta^{18}O$ gradient and the rainfall $\delta^{18}O$ composition for a given location ($\delta^{18}O = -8.48\text{‰}$ measured at 2500 m a.s.l.) (Table 2).

In the sampled springs of the Pineta Valley, the relatively low tritium content could be explained as being due to a greater turnover time of groundwater associated with a relatively large water storage volume or to the existence of a mixing process between the young recharge water and the old melt water coming from the Monte Perdido glacier, which is located in the upper Pineta Valley (Schotterer et al., 1977; Oerter and Ravert, 1982). More research is needed to determine which of these hypotheses or which combination of them operates in the PNOMP. With this purpose, a new field campaign that includes an exhaustive spring inventory and groundwater sampling focused on the Pineta Valley is being conducted.

In the case of the Fuen dero Baño spring (site 22), the relatively low groundwater tritium content and its hydrogeochemical particularities (i.e., the high EC and temperature and the sodium–chloride–sulphate composition) seem to indicate the existence of further water sources contributing to the spring discharge and are especially responsible for the high sulphate content. The monthly averaged sulphate content in rainfall at the meteorological station of Fanlo–Góriz is 1.7 mg/L, so it cannot explain the groundwater sulphate content measured in all of the sampled springs during the last field campaign in September 2013 (Table 5) after applying the correction factor to take into account evaporation and transpiration (Choi et al., 2011).

The use of several isotopes, coupled with hydrogeological and hydrochemical information, has proved to be a useful tool for assessing the origin of solutes. In the case of sulphate, Krouse (1980) suggested that $\delta^{34}\text{S}$ is useful for identifying natural and anthropogenic sources of dissolved sulphate, especially in small study areas, where the sources of dissolved sulphate can be easily distinguished. In addition, numerous studies have used the sulphur isotopic composition coupled with the oxygen isotopic composition of the dissolved sulphate molecule to characterize the sources of dissolved sulphate in surface and groundwater (e.g., Rock and Mayer, 2009; Tichomirowa et al., 2010).

Sulphate in groundwater may have different origins, including: (1) sulphur compounds in bulk atmospheric deposition (rainfall plus dry fallout) entering into the hydrogeological system as rainfall recharge; (2) the oxidation of reduced inorganic S compounds in the terrain (e.g., pyrite); (3) agricultural fertilizers (e.g., $(\text{NH}_4)_2\text{SO}_4$, NPK(S) fertilizers) and the mineralization of soil organic sulphur; and (4) the dissolution of sulphate minerals (e.g., gypsum and/or anhydrite).

There are no measurements of the rainfall $\delta^{34}\text{S}_{\text{SO}_4}$ content in the PNOMP. Querol et al. (2000) and Puig et al. (2008) reported values of +3.0‰ and +3.3‰, respectively, for points located in the eastern zone of the Pyrenean range. These values are within the range of published values (+3‰ to +6‰) for atmospheric sulphate derived from anthropogenic sources (Nriagu and Coker, 1978; Ohizumi et al., 1997; Panettiere et al., 2000; Thode, 1991, among others). The reported rainfall $\delta^{34}\text{S}_{\text{SO}_4}$ values are quite different from the groundwater $\delta^{34}\text{S}_{\text{SO}_4}$ contents measured in the sampled springs (Table 5), which have an average $\delta^{34}\text{S}_{\text{SO}_4}$ value of 16.7‰ with a variation coefficient of 0.001 (Table 5). This result, together with the observed discrepancies between the sulphate content in rainfall and the groundwater samples, shows that rainfall and possibly dry atmospheric deposition are not relevant in accounting for the origin of the groundwater sulphate in the PNOMP.

Sulphide oxidation cannot be the origin of the sulphate due to the disequilibrium between the oxygen isotopic composition of water and sulphate, as can be inferred from Fig. 14-A. The four collected samples are clearly outside the sulphide oxidation field defined by Van Stempvoort and Krouse (1994), which is the zone where the isotopic data should plot if oxygen of sulphate and water are in isotopic equilibrium. Additionally, the PNOMP is a pristine area without agricultural activities, which implies that neither agricultural fertilizers nor soil organic sulphur is responsible for the dissolved sulphate in the groundwater samples.

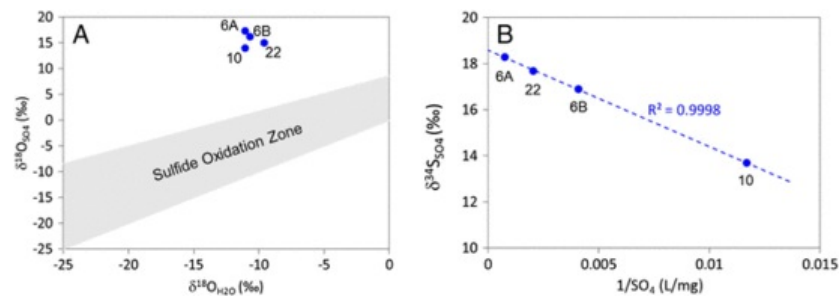


Fig. 14 (A) Isotopic composition of oxygen from dissolved sulphate and groundwater for the sampled springs. The shaded area corresponds to the isotopic sulfide-sulphide oxidation zone defined by Van Stempvoort and Krouse (1994). (B) Plot of $\delta^{34}\text{S}_{\text{SO}_4}$ versus the inverse of SO_4^{2-} . The numbers correspond to those of Table 1.

Evidence for the binary origin of sulphate is provided by the linear relationship between the inverse of the SO_4^{2-} concentration and $\delta^{34}\text{S}_{\text{SO}_4}$ shown in Fig. 14-B, where a linear function fits the measured data with a correlation coefficient $R^2 = 0.9998$. The ends of the line provide information about the isotopic composition of SO_4^{2-} sources (Haefner, 1999; Zuber, 2007; Samborska and Halas 2010). According to the end members, the two sources of dissolved sulphate have isotopic compositions of $\delta^{34}\text{S}_{\text{SO}_4} = +13.7\text{‰}$; $\delta^{18}\text{O}_{\text{SO}_4} = +14.0\text{‰}$ and $\delta^{34}\text{S}_{\text{SO}_4} = +18.3\text{‰}$; $\delta^{18}\text{O}_{\text{SO}_4} = +17.3\text{‰}$, respectively. These values are in agreement with the dissolution of Triassic marine evaporites (Keuper facies). The dissolved sulphate from Fuen Abellá (site 10) is in agreement with the origin of the sulphate from the dissolution of Triassic gypsum, although Triassic evaporite materials do not outcrop in the surroundings of the spring or in the PNOMP, and they do not constitute the detachment material for the tectonic structures in the studied area (see Fig. 1), as they do in other structural units in the Pyrenees. One hypothesis to explain the isotopic composition of the dissolved sulphates in this spring is the existence in the PNOMP area of Eocene sulphate sediments inherited from Triassic evaporites. Sulphate does not fractionate during dissolution, and sulphur isotopes are not greatly fractionated (from 2 to 4‰) by the precipitation of gypsum or anhydrite (Thode and Monster, 1965 and Holser and Kaplan, 1966). In sedimentary transitional environments between marine and continental, due to restriction to the open sea, marine brine compositions may be strongly modified due to freshwater inflows with dissolved sulphate from the dissolution of pre-existing sulphates in outcrops. In this sense, several authors note that upper Eocene evaporite materials from the Ebro basin present a Triassic isotopic composition because it corresponds to the sulphate dissolution of Triassic outcrops and recycling during the upper Eocene sedimentation times (Ayora et al., 1995; Taberner et al., 2000). The coincidence of the sulphate isotopic composition with Triassic values points

to this hypothesis as the most likely, given the geological setting. Nevertheless, more research is needed to determine the presence of recycled evaporites in the Tertiary materials of the PNOMP.

Despite the proximity between Fuen Roya-1 (site 6A) and Fuen Roya-2 (site 6B), both springs show different hydrochemical and isotopic signatures. The groundwater from Fuen Roya-1 is more mineralized and isotopically lighter (i.e., $\delta^{18}\text{O}$, $\delta^2\text{H}$, $\delta^{34}\text{S}_{\text{SO}_4}$ and $\delta^{18}\text{O}_{\text{SO}_4}$) than in Fuen Roya-2. These differences point to the existence of two different flow paths, the longer one discharging in the Fuen Roya-1 spring and the shorter one in the Fuen Roya-2 spring. Moreover, the differences in the $\delta^{34}\text{S}_{\text{SO}_4}$ and $\delta^{18}\text{O}_{\text{SO}_4}$ contents might be due to the existence of a local sulphate reduction process in the discharge point in the Fuen Roya-2 spring. Additionally, the Tertiary sulphate with a recycled isotopic composition from the Triassic might also explain the sulphate isotope value observed in Fuen dero Baño spring (site 22) (Fig. 11).

6 Conclusions

In general, the groundwater in the PNOMP is dominantly of the calcium bicarbonate and calcium–magnesium bicarbonate types, suggesting a dominant calcite dissolution process in agreement with the lithology of its permeable horizons, i.e., upper Cretaceous and lower Paleocene–Eocene limestones, dolomites and calcarenites. The concentrations of these major ions do not present important seasonal content variations. Additionally, the magnesium content in the groundwater at the Ordesa Valley sector increases and the calcium content decreases as the altitude of the sampled points decreases. This is interpreted to result from the existence of a carbonate dissolution process, although more detailed studies are needed. Locally, two other different chemical compositions have been found: (1) a sodium–sulphate–chloride composition in the Fuen dero Baño spring (site 22), with high EC (3580 $\mu\text{S}/\text{cm}$) and temperature (26 °C), interpreted as the mixing of local rainfall recharge and local highly mineralized groundwater flow; and (2) a calcium–sulphate composition in the Fuen Roya (sites 5, 6, 6A and 6B) and Fuen Abellá (site 10) springs.

Rainfall produced by the Atlantic low-pressure fronts appears to be mainly responsible for aquifer recharge. The groundwater isotope ($\delta^{18}\text{O}$ and $\delta^2\text{H}$) composition during the autumn, winter, and spring months presents a deuterium excess with respect to the GMWL, which could be related to the dynamics of the daily cycle of (1) snow sublimation producing deuterium enriched vapour to the local atmosphere during the hours of highest sun irradiation, (2) the mixing of the sublimated vapour with the advected atmospheric water vapour coming from neighbouring lower altitude zones, and (3) the condensation on the higher altitude snow surface of deuterium enriched water vapour due to the low night temperatures. This is a preliminary result to be confirmed with further sampling and consideration of wind conditions, if this can be done.

A local altitudinal isotopic gradient of -0.31‰ $\delta^{18}\text{O}/100\text{ m}$ is obtained for the PNOMP, which allows estimating the average altitude of the recharge areas between 2500 and 3200 m a.s.l. The $\delta^{18}\text{O}$ and $\delta^2\text{H}$ compositions in the springs present a sinusoidal trend throughout the year whose amplitude and time shift for each spring show a linear dependency with the altitude difference between the assumed recharge area and the discharge point of the sampled spring.

The evolution of the $\delta^{18}\text{O}$ and $\delta^2\text{H}$ composition in the sampled springs shows a sinusoidal pattern that reflects the isotope input function entering the system as local recharge (Maloszewski et al., 2002, 1983). The estimated amplitude and the time shift present a linear relationship with the altitude difference ΔZ between the recharge areas and the discharge points of the sampled springs. This illustrates that the isotopic signal of the recharge water is delayed and progressively buffered as the altitude difference of the sampling point increases.

The tritium content in most sampled springs is similar to the values reported for the closest REVIP stations for rainfall during the last 15 years. This result reflects the short residence times of the water recharge through the aquifer, which is coherent with a high karst development. The averaged tritium content of the sampled springs in the PNOMP is 4.9 ± 0.6 TU. Lower values are observed in the Fuen dero Baño spring (site 22) (2.7 ± 0.5 TU), in the Añisclo Valley, and in the Fuen de la Bispeta (site 28) (2.2 ± 0.4 TU) and Fuen el Felcarral (site 27) (1.0 ± 0.4 TU) springs in the Pineta Valley. In the case of the Añisclo Valley, the low tritium values seem to indicate a contribution of thermal, highly mineralized regional groundwater flow to the Fuen dero Baño spring, which is also supported by the hydrogeochemical data and the isotopic composition of the dissolved sulphate. Further studies are needed to resolve the different operational hypotheses regarding the low tritium content in the sampled springs of the Pineta Valley.

The sulphate content measured in the Fuen Roya-1, Fuen Roya-2, Fuen Abellá, and Fuen dero Baño springs could be explained by the dissolution of Eocene evaporitic materials with an isotopic composition inherited from Triassic evaporites. Taking into account such an origin for the sulphate, local sulphate reduction processes might explain the isotopic groundwater composition in some springs. Further research is needed to confirm the existence of these inherited sulphates in the Eocene sedimentary materials of the PNOMP.

The carbonate karstic aquifer of the PNOMP is a very complex hydrological system developed in a high mountain environment. The multidisciplinary approach (geology, geochemistry and environmental isotopes) taken in this study has contributed to the progressive development of a hydrogeological conceptual model of aquifer system functioning.

7 Uncited references

Alealá, 2006

Gantarelli, 2011

Claypool et al., 1980

Goney et al., 1996

Schellart, 2002

Acknowledgements

This research was undertaken as part of the project "Hydrological behaviour analysis of groundwater dependent wetlands", funded by the Geological Survey of Spain (IGME) with reference number CANOA-73.3.00.44.00, and by the Spanish Government CICYT project CGL2011-29975-C04-01 and the Catalan Government project 2014SGR 1456. The authors thank the Ordesa and Monte Perdido National Park Direction (Gobierno de Aragón) and the Pyrenean Institute of Ecology (IPE-CSIC) for their collaboration. Meteorological data have been provided by the Spanish Meteorological Agency (AEMET). The isotopic rainfall data have been provided by the Centro de Estudios de Técnicas Aplicadas (CETA) of the Centro de Estudios y Experimentación de Obras Públicas (CEDEX), which, together with the AEMET, manages the Spanish Monitoring Network for Isotopes in Precipitation (REVIP).

We would also like to thank the anonymous reviewers for their constructive comments and suggestions which led to a substantial improvement of the paper.

References

- AEMET/IM, Atlas Climático Ibérico-Iberian Climate Atlas, 2011, AEMET & IM; Madrid, 1–80.
- Alcalá, F.J., (2006). Recarga a los acuíferos españoles mediante balance hidrogeoquímico. Doctoral dissertation, Technical University of Catalonia (UPC). Barcelona.
- APHA, Standard methods for examination of water and wastewater, In: *17 Ed-American Public Health Association, American Water Works Association, Water Pollution Control Federation*, 1989.
- Araguás-Araguás L., Froehlich K. and Rozanski K., Deuterium and oxygen-18 isotope composition of precipitation and atmospheric moisture, *Hydrol Process* **14**, 2000, 1341–1355.
- Arce M., García M.A. and Arqued V., Caracterización del oxígeno 18, deuterio y tritio en las aguas del Pirineo, In: Medina A. and Carrera J., (Eds.), *Las caras del Agua Subterránea, Congreso en Memoria de Germán Galarza*, 2001, UPC; Barcelona, 387–393.
- Ayora C., Taberner C., Pierre C. and Pueyo J.J., Modeling the sulfur and oxygen isotope composition of sulfates through a halite-potash sequence: implications for the hydrological evolution of the Upper Eocene South Pyrenean Basin, *Geochem Cosmochim Acta* **59**, 1995, 1799–1808.
- Benito Alonso J.L., Vegetación del Parque Nacional de Ordesa y Monte Perdido, **50**, 2006, Publ. Consejo Protección Naturaleza Aragón; Zaragoza.
- Boronina A., Renard P., Balderer W. and Stichler W., Application of tritium in precipitation and in groundwater of the Kouris catchment (Cyprus) for description of the regional groundwater flow, *Appl Geochem* **20**, 2005, 1292–1308.
- Cantarelli, V., (2011). Tectonic-sedimentary burial history and exhumation of the Southern sector of the Central-Western Pyrenees, Spain. Doctoral dissertation, School of Advanced Studies-Doctorate Course in Earth Sciences (XXIII cycle).
- Carreras J. and Santanach P., El hercínico de los Pirineos, In: *Geología de España, Libro Jubilar Rios, JM*, **1**, 1983, Instituto Geológico y Minero de España, 536–549.
- CHE, Catalogación de los acuíferos de la Cuenca del Ebro, In: *Oficina de Planificación Hidrológica*, 1998, Confederación Hidrográfica del Ebro; Zaragoza.
- Choi B.Y., Yun S.T., Mayer B. and Kim K.H., Sources and biogeochemical behavior of nitrate and sulfate in an alluvial aquifer: hydrochemical and stable isotope approaches, *Appl Geochem* **26** (7), 2011, 1249–1260.
- Clark I.D. and Fritz P., *Environmental isotopes in hydrogeology*, 1997, CRC Press.
- Claypool G.E., Holser W.T., Kaplan I.R., Sakai H. and Zak I., The age curves of sulfur and oxygen isotopes in marine sulfate and their mutual interpretation, *Chem Geol* **28**, 1980, 199–260.
- Collins D.N. and Gordon J.Y., Meltwater hydrology and hydrochemistry in snow- and ice-covered mountain catchments, *Nord. Hydrol.* **12**, 1981, 319–334.
- Coney P.J., Muñoz J.A., McClay K.R. and Evenchick C.A., Syntectonic burial and post-tectonic exhumation of the southern Pyrenees foreland fold-thrust belt, *J Geol Soc* **153** (1), 1996, 9–16.
- Cortesi N., Trigo R.M., Gonzalez-Hidalgo J.C. and Ramos A.M., Modelling monthly precipitation with circulation weather types for a dense network of stations over Iberia, *Hydrol Earth Syst Sci* **17** (2), 2013, 665–678.
- Custodio E., Estimation of aquifer recharge by means of atmospheric chloride deposition balance, *Contrib Sci* **6**, 2010, 81r97.

- Díaz-Teijeiro M.F., Rodríguez-Arévalo J. and Castaño S., La Red Española de Vigilancia de Isótopos en la Precipitación (REVIP): distribución isotópica espacial y aportación al conocimiento del ciclo hidrológico, *Ing Civ* **155**, 2009, 87–97.
- Dogramaci S.S., Herczeg A.L., Schiff S.L. and Bone Y., Controls on $d^{34}\text{S}$ and $d^{18}\text{O}$ of dissolved SO_4 in aquifers of the Murray Basin (Australia) and their use as indicators of flow processes, *Appl Geochem* **16**, 2001, 475–488.
- Froehlich K., Kralik M., Papesch W., Rank D., Scheifinger H. and Stichler W., Deuterium excess in precipitation of Alpine regions—moisture recycling, *Isotopes Environ Health Stud* **44** (1), 2008, 1–10, <http://dx.doi.org/10.1080/10256010801887208>.
- García-Ruiz J.M., Valero-Garcés B.L., Beguería S., López-Moreno J.I., Martí-Bono C., Serrano-Muela P., et al., The Ordesa and Monte Perdido National Park, Central Pyrenees, In: *Landscapes and landforms of Spain*, 2014, Springer; Netherlands, 165–172.
- Gonfiantini R., Roche M.A., Olivry J.C., Fontes J.Ch. and Zuppi G.M., The altitude effect on the isotopic composition of tropical rains, *Chem Geol* **181**, 2001, 147–167.
- González-Fernández B., Meléndez-Asensio M. and Menéndez-Casares E., Hydrogeological characterization of carbonated Jurassic aquifers in the Gijón–Villaviciosa basin (Asturias, N Spain) by means of geochemical and isotopic techniques, *Environ Earth Sci* **59** (4), 2009, 913–928.
- Goodess C.M. and Palutikof J.P., Development of daily rainfall scenarios for southeast Spain using a circulation-type approach to downscaling, *Int J Climatol* **18** (10), 1998, 1051–1083.
- Gremaud V. and Goldscheider N., Geometry and drainage of a retreating glacier overlying and recharging a karst aquifer, Tsanfleuron–Sanetsch, *Swiss Alps Acta Carsol* **39** (2), 2010, 289–300.
- Gremaud V., Goldscheider N., Savoy L., Favre G. and Masson H., Geological structure, recharge processes and underground drainage of a glacierised karst aquifer system, Tsanfleuron–Sanetsch, *Swiss Alps Hydrogeol J* **17** (8), 2009, 1833–1848.
- Gustafson J.R., Snowmelt water isotope fractionation in high elevation seasonal snowpacks: implications for isotope hydrograph studies, <http://www.sahra.arizona.edu/unesco/casestudies/WestUS2007/>, (December 2007).
- Haefner R.J., A sulfur isotope mixing model to trace leachate from pressurized, fluidized bed combustion byproduct in an abandoned coal mine setting, In: *International Ash Utilization Symp. Center for Applied Energy Research, University of Kentucky, Paper #280*, 1999, [<http://www.flyash.info>].
- Hannah D.M. and McGregor G.R., Evaluating the impact of climate on snow- and ice-melt dynamics in the Taillon basin, French Pyrenees, *J Glaciol* **43**, 1997, 463–568.
- Holser W.T. and Kaplan I.R., Isotope geochemistry of sedimentary sulfates, *Chem Geol* **1**, 1966, 93–135.
- IGME-OAPN, Guía Geológica del Parque Nacional de Ordesa y Monte Perdido, In: *Guías geológicas de Parques Nacionales*, 2013, Editorial Everest, (214 pp.).
- Iribar V. and Antigüedad I., Definición de zonas de recarga de manantiales kársticos mediante técnicas isotópicas ambientales, In: *Simp. Rec. Hidr. en regiones Kársticas*, **1**, 1996, Gob. Vasco/AIH-GE; Vitoria-Gasteiz, 271–280.
- Jenkinson A. and Collison F., An initial climatology of gales over the North Sea, In: *Synoptic climatology branch memorandum*, **62**, 1977.
- Jódar J., Lambán L.J., Medina A. and Custodio E., Exact analytical solution of the convolution integral for classical hydrogeological lumped-parameter models and typical input tracer functions in natural gradient systems, *J Hydrol* 2014, <http://dx.doi.org/10.1016/j.jhydrol.2014.10.027>.
- Jones P.D., Hulme M. and Briffa K.R., A comparison of lamb circulation types with an objective classification scheme, *Int J Climatol* **13** (6), 1993, 655–663, <http://dx.doi.org/10.1002/joc.3370130606>.
- Kalnay E., Kanamitsu M., Kistler R., Collins W., Deaven D., Gandin L., et al., The NCEP/NCAR 40-year reanalysis project, *Bull Am Meteorol Soc* **77** (3), 1996, 437–471, [[http://dx.doi.org/10.1175/1520-0477\(1996\)077 < 0437:TNYRP > 2.0.CO;2](http://dx.doi.org/10.1175/1520-0477(1996)077<0437:TNYRP>2.0.CO;2)].
- Kiraly L., Modelling karst aquifers by the combined discrete channel and continuum approach, In: *6th conference on limestone hydrology and fissured aquifers: modelling karst aquifers*, 1997, Université de Franche-Comté, Sciences et Technique de l'Environnement; La Chaux-de-Fonds, 1–26.
- Krouse H.R., Sulphur isotopes in our environment, In: Fritz P. and Fontes J.-Ch.J.Ch. (Eds.), *The terrestrial environment, Isotope Geochemistry* vol. **1**, 1980, Elsevier; Amsterdam, 435–471.
- Maloszewski P., Stichler W., Zuber A. and Rank D., Identifying the flow systems in a karstic-fissured-porous aquifer, the Schneesalpe, Austria, by modelling of environmental ^{18}O and ^3H isotopes, *J Hydrol* **256** (1), 2002, 48–59.

- Małoszewski P., Rauert W., Stichler W. and Herrmann A., Application of flow models in an alpine catchment area using tritium and deuterium data, *J Hydrol* **66**, 1983, 319–330, [http://dx.doi.org/10.1016/0022-1694\(83\)90193-2](http://dx.doi.org/10.1016/0022-1694(83)90193-2).
- Motyka J., A conceptual model of hydraulic networks in carbonate rocks, illustrated by examples from Poland, *Hydrogeol J* **6**, 1998, 469–482.
- Muñoz J.A., Evolution of a continental **collision** belt: ECORS-Pyrenees crustal balanced cross-section, In: McClay K.R., (Ed), *Thrust tectonics*, 1992, Chapman & Hall, 235–246.
- Muñoz J.A., Martínez A. and Vergas J., Thrust sequences in the Spanish eastern Pyrenees, *J Struct Geol* **8**, 1986, 399–405.
- Nriagu J.O. and Coker R.D., Isotopic composition of sulphur in precipitation within the Great Lakes Basin, *Tellus* **30**, 1978, 367–375.
- Oerter H. and Ravert W., Core drilling on Vernagtferner (Oetztal Alps, Austria) in 1979: tritium contents, *Z Gletscher Glazialgeol* 1982, **Volume 18-1, 13-22**.
- Ohizumi T., Fukuzaki N. and Kusakabe M., Sulfur isotopic view on the sources of sulfur in atmospheric fallout along the coast of the sea of Japan, *Atmos Environ* **13**, 1997, 1339–1348.
- Panettiere P., Cortecchi G., Dinelli E., Bencini A. and Guidi M., Chemistry and sulfur isotopic composition of precipitation at Bologna, Italy, *Appl Geochem* **15**, 2000, 1455–1467.
- Parish M., A structural interpretation of a section of the Gavarnie nappe and its implications for Pyrenean geology, *J Struct Geol* **6**, 1984, 247–255.
- Peel M.C., Finlayson B.L. and McMahon T.A., Updated world map of the Köppen–Geiger climate classification, *Hydrol Earth Syst Sci* **11**, 2007, 1633–1644, <http://dx.doi.org/10.5194/hess-11-1633-2007>.
- Pérez C., Funcionamiento hidrogeológico de un humedal hipogénico de origen kárstico en las Sierras Marginales Pirenaicas: Las Lagunas de Estaña (Huesca), (PhD. Thesis)2013, Universidad Complutense de Madrid.
- Press W.H., Teukolsky S.A., Vetterling W.T. and Flannery B.P., Numerical recipes in C, 1992, Cambridge University Press.
- Puig R., Avila A. and Soler A., Sulphur isotopes as tracers of the influence of a coal-fired power plant on a Scots pine forest in Catalonia (NE Spain), *Atmos Environ* **42** (4), 2008, 733–745.
- Querol X., Alastuey A., Chaves A., Spiro B., Plana F. and Lopez-Soler A., Sources of natural and anthropogenic sulphur around the Teruel power station, NE Spain, In: *Inferences from sulphur isotope geochemistry, Atmospheric Environment* **34**, 2000.
- Ríos-Aragüés L.M., Introducción al mapa geológico del Parque Nacional de Ordesa y Monte Perdido, In: *Sociedad Española de Espeleología y Ciencias del Karst, Boletín* **5**, 2003, 84–99.
- Rock L. and Mayer B., Identifying the influence of geology, land use, and anthropogenic activities on riverine sulfate on a watershed scale by combining hydrometric, chemical and isotopic approaches, *Chem Geol* **262**, 2009, 121–130.
- Samborska K. and Halas S., ³⁴S and ¹⁸O in dissolved sulfate as tracers of hydrogeochemical evolution of the Triassic carbonate aquifer exposed to intense groundwater exploitation (Olkusz–Zawiercie region, southern Poland), *Appl Geochem* **25**, 2010, 1397–1414, <http://dx.doi.org/10.1016/j.apgeochem.2010.06.010>.
- Sapriza-Azuri G., Jódar J., Carrera J. and Gupta H.V., Stochastic simulation of nonstationary rainfall fields, accounting for seasonality and atmospheric circulation pattern evolution, *Math Geosci* **45** (5), 2013, 621–645.
- Schaefer R.W. and Usdowski E., Application of stable carbon and sulfur isotope models to the development of groundwater in a limestone–dolomite–anhydrite–gypsum area, In: Matthes G.F., Frimmel P., Hirsch H.D., Schulz H.-E. and Usdowski E., (Eds.), *Progress in hydrogeochemistry*, 1992, Springer; Berlin, 157–163.
- Schellart W.P., Analogue modelling of large-scale tectonic processes: an introduction, *J Virtual Explor* **7**, 2002, 1–6.
- Schotterer U., Finkel R., Oeschger H., Siegenthaler U., Wahlen M., Bart G., et al., Isotope measurements on firn and ice cores from alpine glaciers, In: *Isotopes and impurities in snow and ice, Geographica Helvetica* 1977, [<http://www.geogr-helv.net/68/227/2013/gh-68-227-2013.pdf>].
- Seguret M., Étude tectonique des nappes et séries décollées de la partie centrale du versant sud des Pyrénées, *Ser. Geol. Struct.* **2**, 1972, Pub. USTELA; Montpellier.
- Stichler W., Schotterer U., Fröhlich K., Ginot P., Kull C., Gäggeler H., et al., Influence of sublimation on stable isotope records recovered from high-altitude glaciers in the tropical Andes, *J Geophys Res* **106** (D19), 2001, 22,613–22,620.
- Taberner C., Cendón D.I., Pueyo J.J. and Ayora C., The use of environmental markers to distinguish marine vs continental deposition and to quantify the significance of recycling in evaporite basins, *Sediment Geol* **137**, 2000, 213–240.
- Thode H.G., Sulfur isotopes in nature and the environment: an overview, In: Krouse H.R. and Grinenko V.A., (Eds.), *Stable isotopes: natural and anthropogenic sulphur in the environment, SCOPE vol. 43*, 1991, Wiley; Chichester, 1–26.

Thode H.G. and Monster J., Sulfur-isotope geochemistry of petroleum, evaporites and ancient seas, In: Young A. and Galley J.E., (Eds.), *Fluids in subsurface environments*, *Am. Ass. Petrol. Geol. Mem.* **4**, 1965, 367–377.

Tichomirowa M., Heide C., Junghans M., Haubrich F. and Matschullat J., Sulfate and strontium water source identification by O, S and Sr isotopes and their temporal changes (1997–2008) in the region of Freiberg, central-eastern Germany, *Chem Geol* **276**, 2010, 104–118.

Van Stempvoort D.R. and Krouse H.R., Controls of ^{18}O in sulfate: review of experimental data and application to specific environments, In: *ACS symposium series*, *American Chemical Society* vol. **550**, 1994.

Vuille M., Zur raumzeitlichen Dynamik von Schneefall und Ausaperung im Bereich des südlichen Altiplano, Südamerika, *Geogr. Bernensia*, **G45**, 1996, 1–118.

Tracer techniques in hydrogeological investigations, In: Zuber A., (Ed), *Methodological handbook*, 2007, Publishing House of the Wroclaw University of Technology; Wroclaw, [in Polish].

Highlights

- Environmental tracers are essential to study complex alpine karst aquifers.
- The long presence of snow controls the deuterium excess in groundwater.
- Seasonal δD content in springs depends on gap between recharge and discharge points.
- The first hydrogeological characterization of the Ordesa National Park is presented.
- Sulphate content in springs comes from material recycled from Triassic evaporites.

Queries and Answers

Query:

The term “OMPNP” has been changed to “PNOMP”. Please check and amend as necessary.

Answer: OK, PNOMP is the right acronym

Query:

Please provide a definition for the significance of italicized data in Table 2.

Answer: Data which is obtained through a calculation procedure instead of a direct measurement is displayed in the table with an italicized format

Query:

Please identify the corresponding author and provide the correspondence address.

Answer: The corresponding author is J. Jódar

The correspondence address is the following:

Department of Geotechnical Engineering and Geosciences, Technical University of Catalonia (UPC), Barcelona, Spain

Query:

The country name "Spain" has been inserted to the 1st and 3rd affiliations. Please check and amend as necessary.

Answer: In both cases it is right.

Query:

The citation "Collins and Young 1981" has been changed to match the author name/date in the reference list. Please check here and in subsequent occurrences, and correct if necessary.

Answer: As you point the right citation is "Collins and Gordon, 1981). The change is correct. The citation does not appear any more in the manuscript, therefore no more changes are necessary in this regard.

Query:

Please note that Table 4 was not cited in the text. Please check, and correct if necessary.

Answer: You are right. We forgot to cite the Table 4. The point where you have included the citation is not correct. The citation should appear just at the end of the previous paragraph, that is:

Between May 2011 and April 2012, following a monthly schedule, groundwater samples were obtained from six springs (Table 2). In this case, the groundwater samples were only analysed for $\delta^{18}\text{O}$ and $\delta^2\text{H}$ (see Table 4).

Query:

The citation "Iribar et al. (1996)" has been changed to match the author name/date in the reference list. Please check here and in subsequent occurrences, and correct if necessary.

Answer: The change is correct. This citation appears once more in the "Discussion" section but it appears already corrected.

Query:

The citation "Iribar et al. (1996)" has been changed to match the author name/date in the reference list. Please check here and in subsequent occurrences, and correct if necessary.

Answer: The change is correct.

Query:

Uncited references: This section comprises references that occur in the reference list but not in the body of the text. Please position each reference in the text or, alternatively, delete it. Thank you.

Answer: I have deleted the uncited references.

Query:

Please provide the volume number and page range for the bibliography in 'Oerter and Ravert, 1982'.

Answer: Indeed. Volume 18 (1982), Book I, page 13-22

I have included this information in the reference.

Query:

Please confirm that given names and surnames have been identified correctly.

Answer: Yes, all the names have been identified correctly.

Query:

Figure 1 contains substandard texts. Please do not re-use the file that we have rejected or attempt to increase its resolution and re-save. It is originally poor, therefore, increasing the resolution will not solve the quality problem. We suggest that you provide us the original format. We prefer replacement figures containing vector/editable objects rather than embedded images. Preferred file formats are eps, ai, tiff and pdf. For more information, visit Elsevier website at: <http://www.elsevier.com/author-schemas/artwork-and-media-instructions/>.

Answer: We have attached a new version of Figure 1 with a increased resolution